Chin-Yin Hsu[a], Teng-Chun Yang[a], Tung-Lin Wu, Ke-Chang Hung and Jyh-Horng Wu*

The influence of bamboo fiber content on the non-isothermal crystallization kinetics of bamboo fiber-reinforced polypropylene composites (BPCs)

https://doi.org/10.1515/hf-2017-0046
Received March 15, 2017; accepted September 18, 2017; previously published online January 26, 2018

Abstract: Bamboo fiber (BF)-reinforced polypropylene (PP) composites (BPCs) have been investigated and it was shown by differential scanning calorimetry (DSC) that BF is a nucleation agent and accelerates the crystallization rate of the PP matrix. Numerical analyses according to Avrami, Avrami-Ozawa, and Friedman described well the nucleation mechanism, the crystallization rate and the activation energy for the non-isothermal crystallization behavior of BPCs, respectively. The Avrami approach indicated that BF as a reinforcement significantly changed the crystal growth mechanism of PP matrix during the cooling process. Based on the Avrami-Ozawa method, a lower cooling rate can achieve a certain relative crystallinity degree within a time period. According to the Friedman method, the activation energies of BPCs were lower than that of neat PP below a relative crystallinity of 35%, when the BF content was more than 60%.

Keywords: bamboo fiber, bamboo fiber/PP composite (BPC), cooling rate, crystallization kinetics, non-isothermal crystallization, polypropylene (PP)

Introduction

For the last number of decades, wood plastic composites (WPCs) and other natural fiber-reinforced polymers have been increasingly the focus of research interest and have found many applications, although synthetic fibers still dominate the reinforcement industry (Mohanty et al. 2002; Chand and Fahim 2008). It was has long been recognized that bamboo fibers (BFs) have excellent properties and are efficient as reinforcement in polymer composites (Chen et al. 1998; Lee and Ohkita 2004; Lee et al. 2004; Okubo et al. 2004; Takagi and Ichihara 2004; Kitagawa et al. 2005; Chattopadhyay et al. 2011; Wang et al. 2014; Cheng et al. 2015; Yang et al. 2015; Li et al. 2017). Bamboo possesses excellent mechanical properties, because of the longitudinal alignment of fibers with a relatively small microfibril angle (2–10°), and which contain around 60% cellulose and a lot of lignin (Li et al. 2015; Liu et al. 2015, 2016). There are many methods available for isolation of BF, such as alkaline treatment, steam explosion and mechanical methods (Deshpande et al. 2000; Okubo et al. 2004; Das and Chakraborty 2008). According to Das and Chakraborty (2008), the alkaline concentrations between 15 and 20% afford BFs with optimal properties. Deshpande et al. (2000) found that BFs can be isolated by a combination of chemical and mechanical treatments, and the resulting BF-reinforced polymer composites (BPCs) have a high tensile strength. Okubo et al. (2004) reported on the good mechanical properties of BPCs, in which BFs obtained by steam explosion were combined with polypropylene (PP). However, BF isolation is still time-consuming and not always eco-efficient.

In the present study, BFs will be isolated from bamboo shavings and sawdust, which are byproducts of the bamboo-processing industry. To date, the research concerning BPCs has focused primarily on the thermal and mechanical properties of the composites as a function of fiber type, fiber loading, functional additives and fiber modification (Tokoro et al. 2008; Lee et al. 2009; Yang et al. 2015). Another important aspect of this topic was neglected, namely the fact that the semi-crystalline properties of the polymer materials have a big influence on the microstructures and mechanical properties of the end-products along with the thermal and press history of the materials (Kamal and Chu 1983). The practical molding and solidification processes for polymer composites usually proceed under non-isothermal conditions, and the resulting microstructure has a significant effect on the ultimate properties of the product (Shen et al. 2013). Therefore, the non-isothermal crystallization kinetics of polymer composites with natural fibers needs more investigation. Research has been done in this context with fibers of flax, bamboo, kevlar, hemp and kenaf (Arbelaiz et al. 2006; Buzarovska et al. 2006; Phuong and Girbert 2010; Ou et al. 2011; Niu

[a]**Chin-Yin Hsu and Teng-Chun Yang:** These authors contributed equally to this work.
***Corresponding author: Jyh-Horng Wu,** Department of Forestry, National Chung Hsing University, Taichung 402, Taiwan, e-mail: eric@nchu.edu.tw
Chin-Yin Hsu, Teng-Chun Yang, Tung-Lin Wu and Ke-Chang Hung: Department of Forestry, National Chung Hsing University, Taichung 402, Taiwan

et al. 2012). On the other hand, little information is available on the effect of BF content on the non-isothermal crystallization behavior of BPCs.

The main objective of the present study was to examine the crystallization kinetics of BF-PP composites (BPCs) with various amounts of BF content under non-isothermal conditions by differential scanning calorimetry (DSC) analysis. Additionally, the thermal crystallization kinetics was investigated by the Avrami method (Avrami 1939, 1940, 1941), Ozawa method (Ozawa 1971) and the Avrami-Ozawa method (Liu et al. 1997, 1998). The focus was on the nucleation mechanism and the crystallization rate. Moreover, the Friedman method (Friedman 1964) was applied to obtain the activation energy of the non-isothermal crystallization, which was calculated as a function of the degree of relative crystallinity using an iso-conversional approach.

Materials and methods

Materials: Commercially available PP was purchased from Yung Chia Chemical Industries Co., Ltd. (Taipei, Taiwan); melt flow index 4–8 g per 10 min, density 915 kg m^{-3}, m.p. 145°C. The plastic pellets were ground in an attrition mill and the particle size between 20 and 80 mesh (180–850 μm) was collected. BFs were prepared by hammer-milling and the particles were sieved to less than 100 mesh (<149 μm). Five BF/PP ratios (0/100, 20/80, 40/60, 60/40 and 80/20) were prepared (abbreviated as BPC_{20}, BPC_{40}, BPC_{60} and BPC_{80}) by means of a Vortex mixer (Scientific Industries, Bohemia, NY, USA). The BFs were oven-dried (MC < 3%) before preparation of the mixture.

DSC measurement: A total of 4–6 mg BPC was placed in DSC aluminum pans. A PerkinElmer DSC-6 instrument (Beaconsfield, UK) was used under nitrogen purging (20 ml min^{-1}). First the samples were heated from room temperature to 200°C (10°C min^{-1}), and this temperature was held for 5 min. Then, the samples were cooled to 50°C at the cooling rates of 2.5, 5, 10, 15, 20 and 25°C min^{-1}. The exothermic flow was recorded as a function of temperature. The PP crystallinity (X_c) was obtained as a function of the cooling rate:

$$X_c\,(\%) = \frac{\Delta H_m}{\Delta H_m^0 \times W_p} \tag{1}$$

where ΔH_m denotes the melting enthalpy for the sample at a given cooling rate, ΔH_m^0 is the melting enthalpy of 100% crystalline PP, and W_p is % by wt. of the PP in the samples. The ΔH_m^0 value is 209 J g^{-1} (Marinelli and Bretas 2003), which is valid for a fully crystalline PP.

The compression molding process of BPCs (300 mm × 200 mm with thickness of 12 mm) was performed in our laboratory (Figure 1). As is visible, the temperature in the surface layer was reduced from 180 to 50°C with a cooling rate of 44°C min^{-1}, while the cooling rate in the core layer was 22°C min^{-1}. Exothermic reactions were seen in the core layer in the range of 3–5 min, indicating significant crystallization at the indicated cooling rate. Accordingly, the crystallization of the PP matrix in the presence of BF was induced at cooling rates below 25°C min^{-1}.

Based on the Avrami (Eq. 2) and Ozawa (Eq. 3) approaches (quotations above), the crystallization kinetics were calculated:

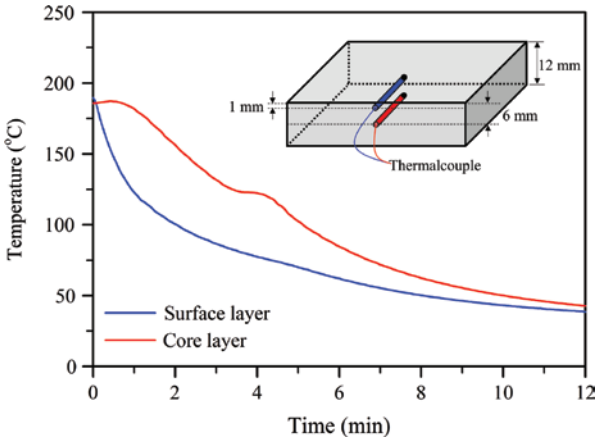

Figure 1: The temperature profiles in the surface and in the core layers of the BPC with 50 wt% fiber during cooling process.

$$X(t) = 1 - \exp(-Kt^n); \tag{2}$$

$$-\ln(1 - X(T)) = \frac{k(T)}{\phi^m} \tag{3}$$

where $X(t)$ is the relative crystallinity at time t; K is the Avrami crystallization rate constant, involving nucleation and growth rate parameters; n denotes a mechanism constant, which depends on the nucleation and growing geometry of the crystallites; $X(T)$ is the relative crystallinity at temperature T; $k(T)$ is the cooling crystallization function; m is the Ozawa exponent, which depends on the nucleation mechanism and the crystal growth; and ϕ is the constant cooling rate. Furthermore, Eqs. (2) and (3) can be converted into Eqs. (4) and (5), respectively, by taking a logarithm of both sides:

$$\log[-\ln(1 - X(t))] = n\log t + \log K; \tag{4}$$

$$\log\{-\ln(1 - X(T))\} = \log k(T) - m\log\phi \tag{5}$$

The non-isothermal crystallization kinetics of some polymer systems are not always described appropriately by the Ozawa equation (see Eder and Wlochowicz 1983; Cebe and Hong 1986; Hao et al. 2010). A combination of the Avrami and Ozawa equations (Liu et al. 1997, 1998) may offer advantages under dynamic crystallization conditions when considered using the cooling crystallization rate ϕ and time t:

$$\ln\phi = \ln F(T) - \alpha\ln t \tag{6}$$

where $F(T) = [k(T)/K]^{1/m}$ denotes the value of the cooling rate at the unit crystallization time under a given degree of crystallinity, and α denotes the ratio of the Avrami exponent n to the Ozawa exponent m.

Moreover, the activation energy of non-isothermal crystallization was calculated according to Friedman (1964):

$$\ln\left(\frac{dX}{dt}\right)_X = \ln(A_X f(X)) - \frac{E_X}{RT_X} \tag{7}$$

where X is the relative degree of crystallinity, t is the time, R is the universal gas constant, $f(X)$ is the function for the reaction mechanism, and A_X, E_X, and T_X are the pre-exponential factors, the activation energy, and the temperature at a given X value, respectively.

Results and discussion

Non-isothermal crystallization behavior

DSC thermograms of neat PP are presented with cooling rates from 2.5 to 25°C min^{-1} in Figure 2a, where the onset temperature (T_o) and the crystallization peak (T_p) are visible. The T_o and T_p points are shifted to lower temperatures and the crystallization profiles are broadened with the increasing cooling rate (Figure 2b and c). For example, the T_p of neat PP decreased from 121.2°C at 2.5°C min^{-1} to 106.6°C at 25°C min^{-1}. The T_o exhibited the same tendency

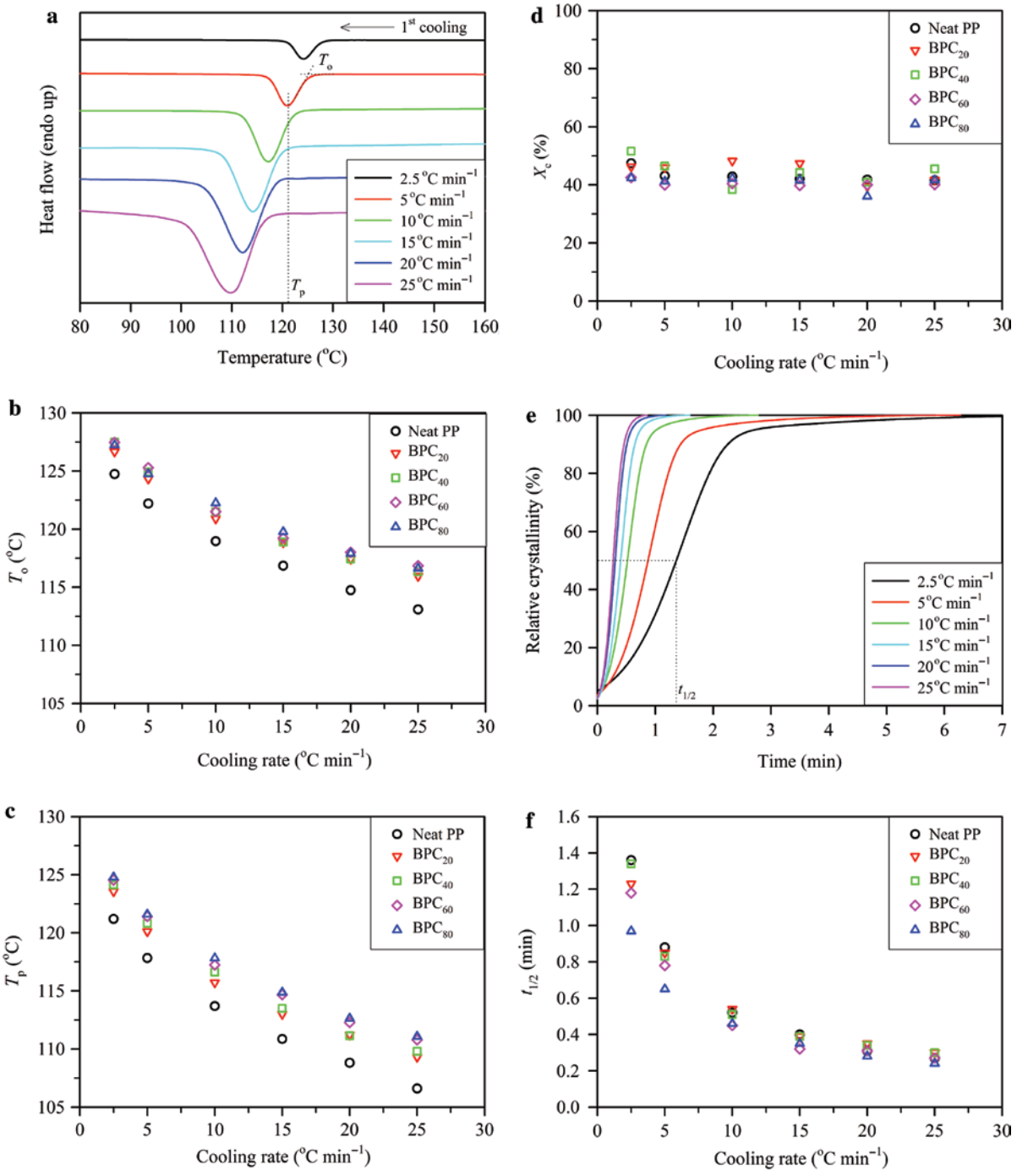

Figure 2: Non-isothermal crystallization behavior of neat PP and BPCs.
(a) DSC thermograms for non-isothermal crystallization of neat PP. (b) The onset temperature (T_o). (c) The crystallization peak (T_p). (d) Crystallinity (X_c) for neat PP and BPCs. (e) Relative crystallinity as a function of time for non-isothermal crystallization of neat PP. (f) The half-time ($t_{1/2}$) as a function of the cooling rate for neat PP and BPCs.

as the T_p. Obviously, at higher cooling rates the motion of PP chains falls behind the cooling rate, and crystallization occurs at lower temperatures. By contrast, at lower cooling rates, sufficient time was available to induce nuclei, resulting in the initiation of crystallization at higher temperatures. The effects of BF contents on the T_o and T_p were also observed. At a given cooling rate, these parameters are in a higher temperature range than that of neat PP, and the temperatures are further shifted with increasing BF contents. To avoid the influence of the cooling procedure, the T_o and T_p from the five cooling rates were calculated as a value, where the cooling rate (ϕ) $\rightarrow 0$, with the help of the exponential decay equation. Accordingly, the fitting of the curves was satisfactory for all samples (R^2 value > 0.99). As listed in Table 1, the T_o and T_p values increased by 2–3°C for BPCs as compared to neat PP. The effect of BF content was not significant. At 25°C min^{-1}, a cooling rate typical of that for the molding process for composites, the T_p increased from 106.6°C (neat PP) to 111.08°C after incorporation of 80% BF into the PP matrix. Apparently, BFs act as a heterogeneous nucleation agent for the PP crystallization of PP with an acceleration effect. On the other hand, the crystallinity (X_c) values for all samples were in the range of 35–55%, i.e. these data are independent of the cooling rate and the BF content (Figure 2d).

Based on the non-isothermal DSC data, the relative crystallinity (X) can be formulated as a function of crystallization temperature, T:

$$X\ (\%) = \int_{T_0}^{T} \left(\frac{dH_c}{dT}\right) dT \Big/ \int_{T_0}^{T_\infty} \left(\frac{dH_c}{dT}\right) dT \tag{8}$$

where T_0 and T_∞ are the onset and offset temperatures of crystallization, and dH_c/dT is the heat flow rate. The crystallization time, t, can be calculated at a given cooling rate:

$$t = (T_0 - T)/\phi \tag{9}$$

where T_0 is the onset temperature at crystallization time $t = 0$, T is the temperature at time t and ϕ is the cooling rate. The X data are presented as a function of crystallization time (t) for neat PP in Figure 2e. The curve is sigmoidal, and this trend was the same for the crystallization curves of all samples at various cooling rates. In summary, there is a lag effect of the cooling rate on crystallization (Phuong and Girbert 2010). Later on, the crystallization rate significantly slowed down due to the impingement of spherulites. The literature has reported (Cebe and Hong 1986; Liu et al. 1997; Regis et al. 2016) that there are two crystallization processes, i.e. the initial fast and the subsequent slow crystallization. At the slower cooling rate, the curve ramp was lower compared to the higher cooling rates, as the crystallization was incomplete. Therefore, the time for complete crystallization decreases with increasing cooling rates. This effect was also quantified by the half-time of crystallization ($t_{1/2}$), which corresponds to 50% X. As shown in Figure 2f, the $t_{1/2}$ values for all samples were reduced (crystallization rates were increased) with increasing cooling rates. The $t_{1/2}$ values for BPCs were significantly lower compared to neat PP, while the effect of BFs are clearly seen in case of lower cooling rates. At the cooling rate of 2.5°C min^{-1}, the $t_{1/2}$ of neat PP was 1.36 min, and $t_{1/2}$ decreased to 0.97 min in the case of 80% BF (BPC_{80}). The $t_{1/2}$ was also extrapolated for neat PP and BPCs based on the exponential decay equation, where ϕ was zero in order to eliminate the influence of the cooling rate as is summarized in Table 1. The $t_{1/2}$ value obviously decreases above 40% BF content. The observations here confirm the literature data (Hao et al. 2010; Phuong and Girbert 2010), according to which BF promotes the crystallization of the PP matrix.

Table 1: The onset temperature (T_o), crystallization peak (T_p) and half-time of crystallization ($t_{1/2}$) of neat PP and BPCs.

Sample codes	Cooling rate (ϕ) $\rightarrow 0$		
	T_o (°C)	T_p (°C)	$t_{1/2}$ (min)
PP	126.9	124.3	2.08
BPC_{20}	129.3	127.1	1.79
BPC_{40}	130.5	127.6	2.20
BPC_{60}	130.6	127.8	1.87
BPC_{80}	129.2	127.8	1.34

The nucleation mechanism by the Avrami method

The nucleation mechanisms have been further analyzed according to Avrami (1939, 1940, 1941). Assuming a constant crystallization temperature, the Avrami model describes well the initial stage of the process. At a given cooling rate, a plot of log[–ln(1 – $X(t)$)] vs. log t leads to the values of n and K (slope of the linear part and intercept), see Eq. (4) and Figure 3a. The log[–ln(1 – $X(t)$)] values in the range of –0.7 to 0.35 correspond to a crystallinity range of 18–89%. The linear regression was perfect with R^2 data >0.99 (Table 2). The fitting lines of each section were nearly parallel for neat PP, implying that the nucleation mechanism and geometries of crystal growth at different cooling rates are similar. The same tendencies for BPCs were observed (not shown). The n values ranged from 2.05 to 2.38 for neat PP at different cooling rates, corresponding

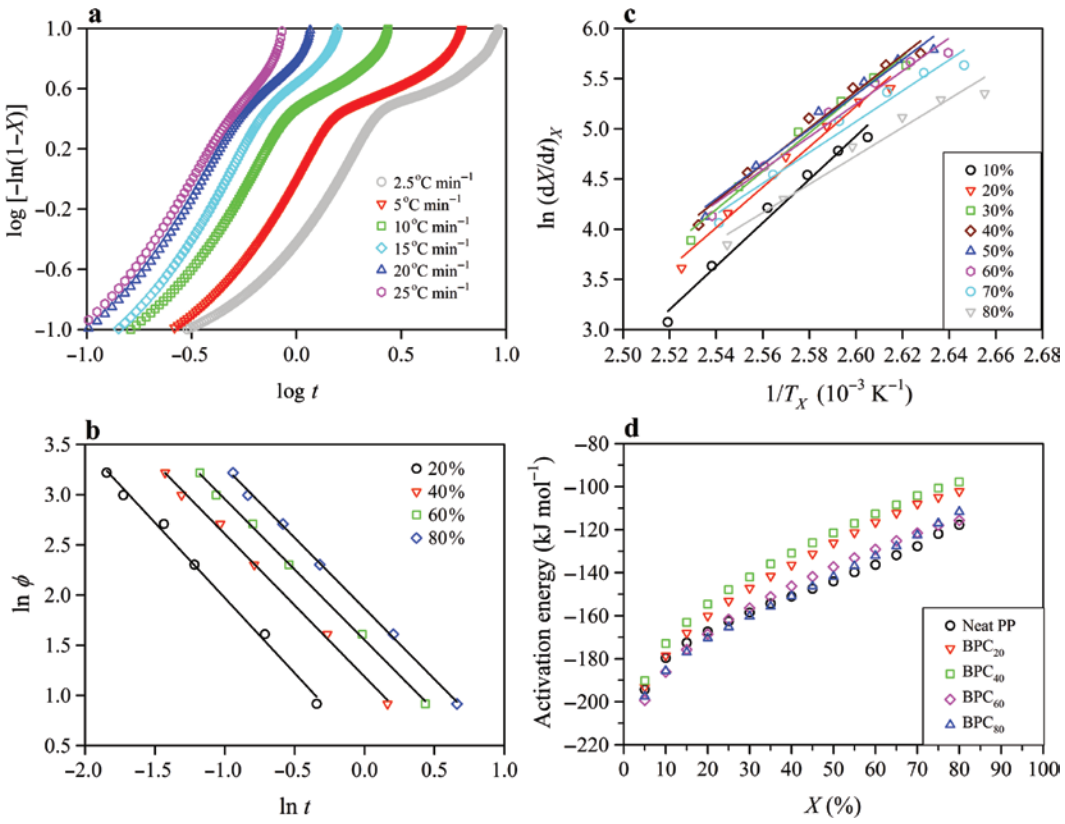

Figure 3: The non-isothermal crystallization kinetics of neat PP.
(a) Avrami plots of log[−ln(1−*X*)] vs. log *t*; (b) Avrami-Ozawa plots of ln ϕ vs. ln *t*; (c) Friedman plots of ln $(dX/dt)_x$ vs. $1/T_x$. (d) Dependence of the effective activation energy on the relative crystallinities for neat PP and BPCs.

to acicular and tabular crystal growth with homogenous nucleation. The following *n* values are seen: 1.93–2.25 for BPC_{20}, 2.05–2.22 for BPC_{40}, 1.83–2.15 for BPC_{60} and 1.57–2.19 for BPC_{80}. These data are lower than those of neat PP, and the range of the *n* value from 1 to 3 is interpreted as being that the non-isothermal crystallization of BPCs is acicular to spherical crystal growth occurs with heterogeneous nucleation. The crystallization rate constant (*K*) was corrected to obtain the crystallization rate (K_J) as a function of cooling rates (ϕ) according to (Jeziorny 1978):

$$\log K_J = \log K / \phi \tag{10}$$

As shown in Table 2, the K_J values for all samples markedly increased with increasing cooling rates up to 10–15°C min^{-1}, and then were slightly reduced above 15°C min^{-1}. Obviously, the highest cold crystallization rate occurs at 10–15°C min^{-1} for neat PP and BPCs. Furthermore, the K_J values of BPCs were higher than that of neat PP, especially at slower cooling rates. For example, at 2.5°C min^{-1}, the K_J for neat PP increased slightly from 0.69 up to 0.91 in case of BPC_{80}. This is manifestation of the promoting effect of BFs to PP crystallization.

The crystallization rate by the Avrami-Ozawa method

According to Eq. (6), $F(T)$ and α can be estimated from the intercept and the slope of a series of straight lines at a given relative crystallinity in the plot of ln ϕ against ln *t*, respectively. The characteristic plot of ln ϕ vs. ln *t* of neat PP is presented in Figure 3b and the corresponding data are listed in Table 3. The data are fitted by a straight line, and the R^2 values >0.99 demonstrate the applicability of this approach. The $F(T)$ for all samples steadily increased with increasing *X*. Accordingly, higher relative crystallinity needs higher cooling rates in the unit crystallization time. The neat PP shows the highest $F(T)$ value, while BPC_{80} the lowest one at a given relative crystallinity. Thus a lower cooling rate can achieve a certain relative crystallinity due to faster crystallization of PP in BPCs. The α coefficient ranges between 1.41–1.50, 1.60–1.72, 1.52–1.56, 1.49–1.55 and 1.61–2.09 for neat PP, BPC_{20}, BPC_{40}, BPC_{60} and BPC_{80} at 20–80% *X*, respectively. The BPC_{80} shows a high α coefficient in the initial stages of crystallization (<40% *X*), confirming the presence of a

Table 2: Parameters calculated based on the Avrami model.

Cooling (°C min^{-1})	K	K_j	n	R^2
PP				
2.5	0.40	0.69	2.05	0.9902
5	0.99	1.00	2.23	0.9950
10	3.24	1.13	2.27	0.9959
15	6.32	1.13	2.38	0.9970
20	10.38	1.12	2.26	0.9973
25	12.87	1.11	2.23	0.9982
BPC_{20}				
2.5	0.49	0.75	1.93	0.9939
5	1.03	1.01	2.25	0.9977
10	2.88	1.11	2.25	0.9984
15	5.55	1.12	2.20	0.9990
20	6.95	1.10	2.16	0.9997
25	9.86	1.10	2.18	0.9996
BPC_{40}				
2.5	0.40	0.69	2.06	0.9959
5	1.09	1.02	2.22	0.9976
10	3.04	1.12	2.18	0.9987
15	5.07	1.11	2.05	0.9983
20	7.04	1.10	2.15	0.9996
25	9.37	1.09	2.12	0.9998
BPC_{60}				
2.5	0.54	0.78	1.83	0.9949
5	1.22	1.04	2.15	0.9976
10	3.32	1.13	1.92	0.9979
15	6.03	1.13	1.88	0.9972
20	8.54	1.11	2.15	0.9996
25	11.33	1.10	2.11	0.9997
BPC_{80}				
2.5	0.79	0.91	1.57	0.9874
5	1.58	1.10	1.76	0.9954
10	3.95	1.15	2.19	0.9989
15	5.96	1.13	2.02	0.9990
20	8.74	1.11	2.00	0.9994
25	13.81	1.11	2.10	0.9997

Table 3: The parameters calculated at various relative crystallinities (X) based on the Avrami-Ozawa model.

X (%)	$F(T)$	α	R^2
PP			
20	1.60	1.50	0.9946
40	3.28	1.42	0.9977
60	4.72	1.40	0.9986
80	6.46	1.41	0.9987
BPC_{20}			
20	1.27	1.72	0.9873
40	2.89	1.60	0.9959
60	4.44	1.59	0.9975
80	6.51	1.60	0.9978
BPC_{40}			
20	1.50	1.56	0.9939
40	2.73	1.52	0.9969
60	4.56	1.52	0.9976
80	6.62	1.54	0.9970
BPC_{60}			
20	1.19	1.55	0.9583
40	2.58	1.50	0.9842
60	3.96	1.49	0.9904
80	5.84	1.49	0.9934
BPC_{80}			
20	0.45	2.09	0.9592
40	1.81	1.73	0.9933
60	3.17	1.64	0.9977
80	5.01	1.61	0.9987

fast initial crystallization regime for a low degree of relative crystallinity.

Crystallization activation energy by the Friedman method

The method of Kissinger (1956) is frequently tested for estimation of the crystallization activation energy for a non-isothermal process (Phuong and Girbert 2010; Ding et al. 2014). However, Vyazovkin (2002) demonstrated that this approach is not suited to non-isothermal cooling processes. This is the reason why the Friedman method was applied in the present study. Figure 3c illustrates the ln $(dX/dt)_X$ vs. $1/T_X$ plot for neat PP at different relative crystallinities. The activation energies for the crystallization process at a given relative crystallinity can be obtained from the slope of the straight line according to the Eq. (7). The plots are shown in Figure 3d. As visible, E_X increased from –194, –193, –190, –199 and –198 kJ mol^{-1} to –118, –102, –98, –116 and –112 kJ mol^{-1}, with increasing X from 5% to 80%, for neat PP, BPC_{20}, BPC_{40}, BPC_{60} and BPC_{80}, respectively. Accordingly, the crystallization process easily proceeded in the beginning but slowed down at higher crystallinity degrees (Run et al. 2007). In the case of BF contents <40%, E_X values are higher compared to neat PP. Thus BF contents below 40% enhance the crystallization energy barrier of PP crystallization. If the BF content >60%, the E_X values are similar to that of neat PP. Lower E_X values were obtained compared to neat PP, when X is lower than 20% and 35% for BPC_{60} and BPC_{80}, respectively. Also these results confirm that BFs act as a heterogeneous nucleation agent promoting the crystallization of PP.

Conclusions

As indicated by the Avrami method, BFs as reinforcements in PP significantly changed the nucleation mechanism of

the PP matrix. The Avrami-Ozawa method shows the PP matrix required a lower cooling rate to reach a certain crystallinity in the presence of BF. The iso-conversional Friedman method reveals similar activation energies of BPCs with BF contents >60% and neat PP. When the relative crystallinity is lower than 20 and 35% for BPC_{60} and BPC_{80}, respectively, their activation energies were lower than that of neat PP, i.e. the BF content affects the crystallization rate of PP. Additionally, the cooling rate is also very influential. The observed parameters could be useful for optimization of the production of BPCs.

Acknowledgment: This work was financially supported by a research grant from the Ministry of Science and Technology, Taiwan (grant no. MOST 105-2628-B-005-002-MY3).

Author contributions: All the authors have accepted responsibility for the entire content of this submitted manuscript and approved submission.
Research funding: The Ministry of Science and Technology of Taiwan (MOST 105-2628-B-005-002-MY3).
Employment or leadership: None declared.
Honorarium: None declared.

References

Arbelaiz, A., Fernández, B., Ramos, J. A., Mondragón, I. (2006) Thermal and crystallization studies of short flax fibre reinforced polypropylene matrix composites: effect of treatments. Termochim. Acta. 440:111–121.

Avrami, M. (1939) Kinetics of phase change. I: general theory. J. Chem. Phys. 7:1103–1112.

Avrami, M. (1940) Kinetics of phase change. II: transformation-time relations for random distribution of nuclei. J. Chem. Phys. 8:212–224.

Avrami, M. (1941) Kinetics of phase change. III: granulation, phase change, and microstructure. J. Chem. Phys. 9:177–184.

Buzarovska, A., Bogoeva-Gaceva, G., Grozdnov, A., Avella, M. (2006) Crystallization behavior of polyhydroxybutyrate in model composites with kenaf fibers. J. Appl. Polym. Sci. 102:804–809.

Cebe, P., Hong, S. D. (1986) Crystallization behaviour of poly(ether-ether-ketone). Polymer 27:1183–1192.

Chand, N., Fahim, M. Tribology of natural fiber polymer composites. Woodhead Publishing, Cambridge, 2008.

Chattopadhyay, S. K., Khandal, R. K., Uppaluri, R., Ghoshal, A. K. (2011) Bamboo fiber reinforced polypropylene composites and their mechanical, thermal, and morphological properties. J. Appl. Polym. Sci. 119:1619–1626.

Chen, X., Guo, Q., Mi, Y. (1998) Bamboo fibre-reinforced polypropylene composite: a study of the mechanical properties. J. Appl. Polym. Sci. 69:1891–1899.

Cheng, H., Gao, J., Wang, G., Shi, S. Q., Zhang, S., Cai, L. (2015) Enhancement of mechanical properties of composites made of calcium carbonate modified bamboo fibers and polypropylene. Holzforschung 69:215–221.

Das, M., Chakraborty, D. (2008) Evaluation of improvement of physical and mechanical properties of bamboo fibres due to alkali treatment. J. Appl. Polym. Sci. 107:522–527.

Deshpande, A. P., Bhaskar Rao, M., Laksjmana Rao, C. (2000) Extraction of bamboo fibers and their use as reinforcement in polymeric composites. J. Appl. Polym. Sci. 76:83–92.

Ding, Q., Zhang, Z., Wang, C., Jiang, J., Li, G., Mai, K. (2014) Non-isothermal crystallization kinetics and morphology of wollastonite-filled β-isotactic polypropylene composites. J. Therm. Anal. Calorim. 115:675–688.

Eder, M., Wlochowicz, A. (1983) Kinetics of non-isothermal crystallization of polyethylene and polypropylene. Polymer 24:1593–1595.

Friedman, H. L. (1964) Kinetics of thermal degradation of char-forming plastics from thermogravimetry. Application to a phenolic plastic. J. Polym. Sci. Polm. Symp. 6:183–195.

Hao, W., Yang, W., Cai, H., Huang, Y. (2010) Non-isothermal crystallization kinetics of polypropylene/silicon nitride nanocomposites. Polym. Test. 29:527–533.

Jeziorny, A. (1978) Parameters characterizing the kinetics of the non-isothermal crystallization of poly(ethylene terephthalate) determined by D. S. C. Polymer 19:1142–1144.

Kamal, M. R., Chu, E. (1983) Isothermal and nonisothermal crystallization of polyethylene. Polym. Eng. Sci. 23:27–31.

Kissinger, H. E. (1956) Variation of peak temperature with heating rate in differential thermal analysis. J. Res. Nat. Inst. Stand. Technol. 57:217–221.

Kitagawa, K., Ishiaku, U. S., Mizoguchi, M., Hamada, H. (2005) Bamboo-based ecocomposites and their potential applications. In: Natural Fibres, Biopolymers, and Biocomposites. Eds. Mohanty, A. K., Misra, M., Drzalv, L. T. CRC Press, Florida.

Lee, S.-H., Ohkita, T. (2004) Bamboo fiber (BF)-filled poly(butylenes succinate) bio-composite – Effect of BF-e-MA on the properties and crystallization kinetics. Holzforschung 58:537–543.

Lee, S.-H., Ohkita, T., Kitagawa, K. (2004) Eco-composite from poly(lactic acid) and bamboo fiber. Holzforschung 58:529–536.

Lee, S. Y., Chun, S. J., Doh, G. H., Kang, I. A., Lee, S., Paik, K. H. (2009) Influence of chemical modification and filler loading on fundamental properties of bamboo fibres reinforced polypropylene composites. J. Compos. Mater. 43:1639–1657.

Li, Y., Yin, L., Huang, C., Meng, Y., Fu, F., Wang, S., Wu, Q. (2015) Quasi-static and dynamic nanoindentation to determine the influence of thermal treatment on the mechanical properties of bamboo cell walls. Holzforschung 69:909–914.

Li, Y., Huang, C., Wang, L., Wang, S., Wang, X. (2017) The effects of thermal treatment on the nanomechanical behavior of bamboo (*Phyllostachys pubescens* Mazel ex H. de Lehaie) cell walls observed by nanoindentation, XRD, and wet chemistry. Holzforschung 71:129–135.

Liu, T., Mo, Z., Wang, S., Zhang, H. (1997) Nonisothermal melt and cold crystallization kinetics of poly(aryl ether ether ketone ketone). Polym. Eng. Sci. 37:568–575.

Liu, T., Mo, Z., Zhang, H. (1998) Nonisothermal crystallization behavior of a novel poly(aryl ether ketone): PEDEKmK. J. Appl. Polym. Sci. 67:815–821.

Liu, H., Jiang, Z., Fei, B., Hse, C., Sun, Z. (2015) Tensile behaviour and fracture mechanism of moso bamboo (*Phyllostachys pubescens*). Holzforschung 69:47–52.

Liu, H., Wang, X., Zhang, X., Sun, Z., Jiang, Z. (2016) In situ detection of the fracture behaviour of moso bamboo (*Phyllostachys pubescens*) by scanning electron microscopy. Holzforschung 70:1183–1190.

Marinelli, A. L., Bretas, R. E. S. (2003) Blends of polypropylene resins with a liquid crystalline polymer, I. Isothermal crystallization. J. Appl. Polym. Sci. 87:916–930.

Mohanty, A. K., Misra, M., Drzal, L. T. (2002) Sustainable biocomposites from renewable resources: opportunities and challenges in the green materials world. J. Polym. Environ. 10:19–26.

Niu, P., Wang, X., Liu, B., Long, S., Yang, J. (2012) Melting and nonisothermal crystallization behavior of polypropylene/hemp fiber composites. J. Compos. Mater. 46:203–210.

Okubo, K., Fujii, T., Yamamoto, Y. (2004) Development of bamboo-based polymer composites and their mechanical properties. Compos. Part A-Appl. S. 35:377–383.

Ou, R., Guo, C., Xie, Y., Wang, Q. (2011) Non-isothermal crystallization kinetics of kevlar fiber-reinforced wood flour/HDPE composites. Bioresources 6:4547–4565.

Ozawa, T. (1971) Kinetics of non-isothermal crystallization. Polymer 12:150–158.

Phuong, N. T., Girbert, V. (2010) Non-isothermal crystallization kinetics of short bamboo fiber-reinforced recycled polypropylene composites. J. Reinf. Plast. Compos. 28:1–16.

Regis, M., Zanetti, M., Pressacco, M., Bracco, P. (2016) Opposite role of different carbon reinforcements on the non-isothermal crystallization behavior of poly(etheretherketone). Mater. Chem. Phy. 179:223–231.

Run, M., Song, H., Yao, C., Wang, Y. (2007) Crystal morphology and nonisothermal crystallization kinetics of short carbon fiber/poly(trimethylene terephthalate) composites. J. Appl. Polym. Sci. 106:868–877.

Shen, H., Xie, B., Yang, W., Yang, M. (2013) Non-isothermal crystallization of polyethylene blends with bimodal molecular weight distribution. Polym. Test. 32:1385–1391.

Takagi, H., Ichihara, Y. (2004) Effect of fibre length on mechanical properties of green composites using starch-based resin and short bamboo fibres. JSME Int. J. 47:551–555.

Tokoro, R., Vu, D. M., Okubo, K., Tanaka, T., Fujii, T., Fujiura, T. (2008) How to improve mechanical properties of polylactic acid with bamboo fibers. J. Mater. Sci. 43:775–787.

Vyazovkin, S. (2002) Is the Kissinger equation applicable to the processes that occur on cooling? Macromol. Rapid. Commun. 23:771–775.

Wang, H., An, X., Li, W., Wang, H., Yu, Y. (2014) Variation of mechanical properties of single bamboo fibers (*Dendrocalamus latiflorus* Munro) with respect to age and location in culms. Holzforschung 68:291–297.

Yang, T.-C., Wu, T.-L., Hung, K.-C., Chen, Y.-L., Wu, J.-H. (2015) Mechanical properties and extended creep behavior of bamboo fiber reinforced recycled poly(lactic acid) composites using the time-temperature superposition principle. Constr. Build. Mater. 93:558–563.